LANGMUIR

Article

pubs.acs.org/Langmuir

Liquid–Liquid Phase Separation in Oligomeric Peptide Solutions

Ying Wang,*[,†,§] Aleksey Lomakin,[†] Sonoko Kanai,[‡] Rainer Alex,[‡] and George B. Benedek[†]

[†]Department of Physics, Massachusetts Institute of Technology, 77 Massachusetts Avenue, Cambridge, Massachusetts 02139, United States

[‡]Roche Pharmaceutical Research and Early Development, Roche Innovation Center Basel, F. Hoffmann–La Roche, Ltd., Grenzacherstrasse 124, CH-4070 Basel, Switzerland

Supporting Information

ABSTRACT: Oligomeric peptides exist widely in living organisms and play a role in a broad range of biological functions. We report the first observation of liquid–liquid phase separation (LLPS) in peptide solutions, in particular, solutions of peptides consisting of noncovalent oligomers. We determined the binary phase boundary of the oligomeric peptide solution and compared the result to the well-established phase diagram of globular proteins. We also provide simple theoretical interpretations of the similarities and differences between the phase diagrams of peptides and proteins. Finally, by tuning inter-oligomer interactions using a crowding agent, we demonstrated that LLPS is a universal phenomenon that can be observed under different solution conditions for a variety of peptides.

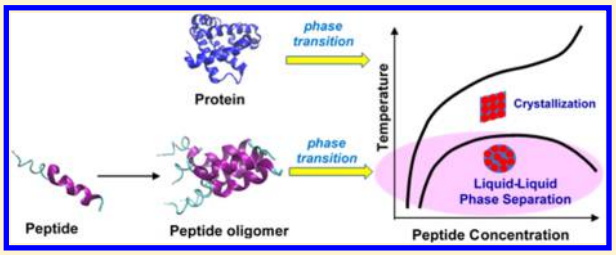

INTRODUCTION

Globular proteins in aqueous solutions can undergo two basic types of phase transitions: crystallization and liquid–liquid phase separation (LLPS).[1,2] The phase transitions of protein solutions underlie the mechanisms of various protein condensation diseases, such as cataracts, sickle cell anemia, and cryoglobulinemia.[3−6] In addition, phase transitions and the closely related nonequilibrium aggregation and gelation phenomena are of increasing interest to the pharmaceutical industry, because of concerns about the solution stability of antibodies and other protein therapeutics.[7,8] In structural biology, protein crystallization is the bottleneck of X-ray crystallographic studies of protein structure–function relationships.[9] Furthermore, the LLPS of protein solutions play a role in normal cellular functions.[10−12] Despite the vast numbers of different proteins and solution conditions in various applications, most globular-protein solutions exhibit similar phase behavior, which can be described by a typical phase diagram with an upper critical temperature.[13] In such phase diagrams, the liquid–liquid binary coexistence curve is located at temperatures lower than the crystallization solubility line (i.e., the liquid–liquid phase transition is metastable, with respect to the liquid–solid phase transition).[13,14] Moreover, the coexistence curves of proteins are often substantially broader than predicted by the mean-field theory. These common features of protein phase diagrams originate from the intrinsic short-range and aeolotopic nature of the interprotein interactions.[13,15] Because of the large size of protein molecules (nanometers), their phase diagrams resemble phase diagrams of colloidal particles.[13,16]

Peptides of less than 50 amino acid residues are ubiquitously endogenous hormones, natural antibiotics, and venoms.[17−20] Bioactive peptides have also inspired the synthesis of biomimetic therapeutics. For small polypeptides with molecular weights under 5000 Da, the range of intermolecular interactions may no longer be considered short, with respect to the size of the polypeptide. Thus, peptides may exhibit phase behavior that is intermediate between that of proteins and small molecules.

In addition, many peptides contain both hydrophilic and hydrophobic amino acids.[21] Unlike proteins, peptides are often not large enough to form compact structures in which hydrophobic amino acids are packaged in cores. Instead, amphiphilic peptides commonly form oligomers.[21−23] The sizes of these peptide oligomers can be comparable to those of proteins. However, major differences may exist between the structures of peptide oligomers and individual proteins.[23] For example, peptide oligomers should be less compact than globular proteins and have more symmetric structures than proteins, because of the presence of identical constituent monomeric peptide units. From a theoretical perspective, the phase behavior of peptide solutions is of fundamental interest for biophysical chemistry.

In this work, we report LLPS in solutions of a series of pharmaceutical peptides, including six palmitoylated incretin peptides, one unconjugated incretin peptide, and the anti-HIV peptide enfuvirtide. All of these peptides form oligomers in aqueous solutions. We study the phase diagrams of these peptides and compare them to the well-established protein phase diagram. By tuning interoligomer interactions using a polymer crowding agent, we show that LLPS occurs in solutions of all of these peptides and at different pH values. This study suggests that phase transitions are ubiquitous and

Received: May 20, 2017
Revised: July 7, 2017
Published: July 10, 2017

DOI: 10.1021/acs.langmuir.7b01693
Langmuir 2017, 33, 7715−7721

fundamental physical changes in peptide solutions. Based on our results, phase transitions are more likely to occur at high peptide concentrations and in crowded solution environments and may alter the classic paradigm of the biological activity of peptides under these conditions.

MATERIALS AND METHODS

Materials and Solution Preparations. We used eight pharmaceutical peptides: seven hybrid incretin peptides used in the treatment of diabetes and one anti-HIV retroviral peptide (enfuvirtide). The primary structures of the eight peptides are shown in Table S1 in the Supporting Information. The seven incretin peptides, which are designated as IP0−IP6, were used in our previous study.[24] The lyophilized peptides (IP0−IP6 and enfuvirtide) were purchased from CS Bio Co. (Menlo Park, CA) through their custom peptide synthesis service and were used without further purification. All peptides had purities of >96%, as determined by reverse-phase high-performance liquid chromatography (HPLC) with a C8 column. The molecular weights of the monomeric peptides were confirmed by mass spectrometry and are 4339 g/mol for IP0, 4706 g/mol for IP1, 4732 g/mol for IP2, 4672 g/mol for IP3, 4697 g/mol for IP4, 4544 g/mol for IP5, 4892 g/mol for IP6, and 4491 g/mol for enfuvirtide. The isoelectric points (IPs) of the peptides were determined by capillary electrophoresis to be pH 4.5 for IP1, 3.6 for IP2, 3.7 for IP3, 4.4 for IP4, 4.0 for IP5, 3.8 for IP6, and 4.8 for enfuvirtide. Polyethylene glycol (PEG) with an average molecular weight of 3350 g/mol was purchased from Sigma−Aldrich (St. Louis, MO).

To prepare the peptide stock solutions, solid peptides were dissolved in phosphate-buffered saline (PBS) prepared with NaH_2PO_4 (Mallinckrodt Chemicals, St. Louis, MO), KH_2PO_4, KCl, and NaCl (Sigma−Aldrich, St. Louis, MO). The pH of the solutions was adjusted to 9 using 1 M sodium hydroxide to facilitate the dissolution of the peptides and then to the desired pH value using 1 M phosphoric acid. The peptide concentration was measured using an ultraviolet (UV) spectrophotometer (DU640, Beckman Coulter, Brea, CA). The extinction coefficients of the peptides at 280 nm were calculated from their respective amino acid sequences, using the ProtParam tool on ExPASy (www.expasy.org) and were adjusted by their total molecular weights to give ε_{280} = 1.96 L/(g cm) for IP0, 1.80 L/(g cm) for IP1, 2.11 L/(g cm) for IP2, 1.82 L/(g cm) for IP3, 1.81 L/(g cm) for IP4, 1.54 L/(g cm) for IP5, 1.75 L/(g cm) for IP6, and 4.04 L/(g cm) for enfuvirtide. The PEG stock solutions were prepared by dissolving PEG in PBS and adjusting the pH to the desired value. The weight fractions of PEG in the stock solutions were calculated from the weights of PEG and buffer.

The density of IP5 solutions at 20 °C (ρ) was determined as a function of peptide concentration (c), using a densitometer (Model DMA 4500, Anton Paar). The partial specific volume of the peptide in PBS ($\bar{v}$) was then calculated using the equation

$$\rho = (1 - v\bar{\rho}_0)c + \rho_0$$

where ρ_0 = 1.005 g/mL is the density of PBS at 20 °C.

Observation of LLPS and Determination of the Phase Diagram. The peptide samples were prepared by mixing the peptide and PEG stock solutions. The concentrations of the peptide and PEG in the samples were calculated using the concentrations and weights of the stock solutions. The samples were homogeneous at room temperature and underwent LLPS when the temperature decreased below a well-defined phase-separation temperature.

We conducted clouding experiments to determine the temperature−concentration phase boundaries of LLPS in the peptide solutions. In a typical clouding measurement, the sample was placed in the temperature-controlled chamber of a custom-built light-scattering apparatus. A laser beam was directed through the sample, and the transmitted light intensity was recorded by a photodiode and a power meter. The temperature was gradually decreased until the transmitted light intensity exhibited an abrupt drop. The clouding of the sample indicated the formation of peptide-rich droplets. The clouding temperature was taken as the phase-separation temperature.

We also conducted solubility measurements to study LLPS in the peptide solutions. This method was previously used to investigate phase separation in antibody solutions.[25] The results obtained via the solubility and clouding measurements are equivalent.[25] In our laboratory setup, the solubility experiments allowed us to measure multiple samples simultaneously. In the solubility measurements, we incubated the samples at a constant temperature (5 °C) for 1 day to achieve equilibrium. The samples became cloudy upon quenching to 5 °C. At the end of the incubation period, the peptide-rich droplets settled to the bottom of the glass test tube and became invisible to the naked eye, whereas the supernatants became transparent. The peptide concentrations in the supernatants were measured by UV absorbance.

Light Scattering. In quasi-elastic light-scattering experiments, 100 μL samples were filtered through a 22 nm syringe filter (Whatman, Anotope, GE Healthcare) and placed in a custom-built, temperature-controlled, light-scattering apparatus employing a He−Ne laser (35 mW, 632.8 nm; Coherent, Inc., Santa Clara, CA) and a correlator (Model PD2000 DLS PLUS, Precision Detectors, Bellingham, MA). All experiments were conducted at a 90° scattering angle. The correlation functions were analyzed using a regularization algorithm (Precision Deconvolve 5.5 software, Precision Detectors) to calculate the distribution of the apparent diffusion coefficient (D). The apparent hydrodynamic radius (R_h) was calculated from D using the Stokes−Einstein equation:

$$R_h = \frac{kT}{6\pi\eta D}$$

The viscosity (η) value of PBS, at 21.0, 26.9, 32.4, and 36.9 °C, were 0.98, 0.85, 0.76, and 0.69 cP, respectively, as determined using a glass capillary viscometer (Model A223, Cannon, State College, PA).

Static light-scattering measurements were collected using a DynaPro NanoStar light-scattering instrument (Wyatt Technology, Goleta, CA) with a 633 nm laser. The scattered intensities of peptide samples with varying concentrations were measured at 25 °C and a fixed angle of 90°. The excess Rayleigh ratio at 90° for the IP5 oligomer was calculated using the relation

$$R_{90^\circ} = R_{90^\circ_r}\left(\frac{n_0^2}{n_r^2}\right)\left(\frac{I_s - I_{s,0}}{I_{s,r}}\right)$$

where n_0 is the refractive index (n_0 = 1.333) and $I_{s,0}$ is the measured scattering intensity of the blank buffer at 25 °C. $R_{90^\circ_r}$ is the Rayleigh ratio at 90° ($R_{90^\circ_r} = 1.359 \times 10^{-5}$ cm^{-1}), n_r is the refractive index (n_r = 1.492),[26] and $I_{s,r}$ is the measured scattering intensity of toluene (the standard). The average molecular weight (M) of the IP5 oligomer was obtained as $Kc/R_{90^\circ} = 1/M + 2B_2c$, where c is the peptide concentration, and K is the optical coefficient, which is defined as

$$K = 4\pi^2 n_0^2\left[\frac{(dn/dc)^2}{N_A\lambda^4}\right]$$

where N_A is Avogadro's number and λ is the wavelength of the laser in a vacuum. The refractive index increment associated with the lipidated peptide concentration—dn/dc = 0.1820 mL/g—was determined previously.[24]

RESULTS AND DISCUSSION

Comparison of LLPS in Peptide and Protein Solutions. We observed LLPS in solutions of an incretin analogue lipopeptide (referenced here as IP5; molecular weight = 4.5 kDa and pI = 4.0; see Table S1 in the Supporting Information for the primary structure of this peptide). Solutions of this peptide at pH 5.5 became cloudy when the temperature was lowered below a certain value and became clear again when the solutions were heated. Under a light microscope, we observed small liquid droplets that appeared viscous but coalesced when pressed under a microscope coverslip (see Figure 1, inset). To further investigate this phenomenon, we determined the phase

DOI: 10.1021/acs.langmuir.7b01693
Langmuir 2017, 33, 7715−7721

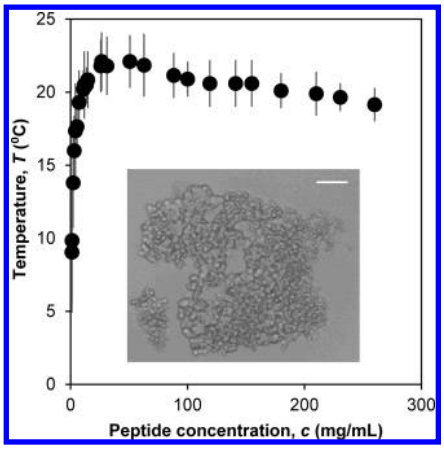

Figure 1. Coexistence curves of LLPS in solutions of an incretin peptide (IP5) at pH 5.5. Vertical bars indicate the temperature hysteresis between the clouding and clearing of the solutions. Inset shows a bright-field microscope image of the peptide-rich liquid condensed phase formed in a 30-mg/mL peptide solution at 21 °C. The white scale bar in the upper right corner represents 10 μm.

boundary (the so-called coexistence curve) for this peptide (i.e., the temperature below which phase separation occurs as a function of the peptide concentration) (see Figure 1).

The coexistence curve of the peptide in Figure 1 has a parabola-like shape, similar to that observed for protein solutions. A close comparison of the coexistence curves of peptides and proteins revealed strikingly different features. The maximum point of the peptide coexistence curve (the critical point) is located at a mass concentration of ~50 mg/mL. The experimental specific volume of the peptide ($\bar{v}$) is equal to 0.708 mL/g, which is consistent with the typical density of protein molecules (i.e., 1.4 g/mL[27]). With $\bar{v}$ = 0.708 mL/g, the critical concentration (50 mg/mL) corresponds to a volume fraction of 3.6%. This apparent peptide critical volume fraction is much lower than that of proteins. In Table 1, we compare the apparent critical volume fraction (ϕ_c^{app}) of the incretin peptide IP5 with the previously reported ϕ_c^{app} values of various proteins and the theoretical values for spherical particles with attractive interactions.

Table 1. Theoretical and Experimental Values of the Apparent Critical Volume Fraction (ϕ_c^{app})[a]

	ϕ_c^{app}	ref
incretin peptide (IP5)	0.036	
immunoglobulins (IgG2-A, IgG2, and IgG1)	0.063	8
spherical particles with very *long* interaction ranges	0.13	13
human lens γD Crystallin	0.13	8
chicken egg white lysozyme	0.16	28
bovine lens γ Crystallins (including γB, γC, γD, and γE)	0.21	29
spherical particles with very *short* interaction ranges	0.27	13

[a]The ϕ_c^{app} values of various proteins and the theoretical values for spherical particles are taken from the references.

To understand the low apparent critical volume fraction of the peptide, we re-examined our understanding of near-spherical proteins. Depending on the range of the attractive interaction, the theoretical ϕ_c value of spherical particles can vary from 0.13 for mean-field interactions to 0.266 for the adhesive sphere model.[13] Table 1 shows that near-spherical proteins, such as lysozyme[28] and eye lens Crystallins,[29] have apparent critical volume fractions ranging from 0.13 to 0.21. However, typical interprotein interactions, such as electrostatic interactions and hydrophobic interactions, are expected to have short ranges under the buffer conditions (short Debye length) used in the studies referenced in Table 1. Therefore, the variation in ϕ_c of near-spherical proteins is unlikely to be attributable to the ranges of interprotein interactions. A simple alternative explanation is that these proteins differ in their specific exclusion volume (EV_s), which is the volume per unit mass of protein inaccessible to other protein molecules. Indeed, experimental studies have shown that proteins can have different densities[27] and, thus, different EV_s values. Table 1 shows that IgG immunoglobulins[8] have ϕ_c^{app} values that are much lower than the mean-field sphere value of 0.13. Unlike near-spherical proteins, IgG has a flexible Y-like trimeric shape. The small apparent critical volume fraction of IgG immunoglobulins is attributable to large EV_s values (i.e., low density proteins). This assumption is consistent with the X-ray crystal structure of IgG, in which the Fab and Fc domains consist of loops formed between light and heavy chains.[30−32] In Table 1, the incretin peptide has even smaller apparent volume fraction than IgG: ϕ_c^{app} = 0.036. As discussed above for proteins, a small ϕ_c^{app} suggests that the peptide is loosely packed in solution and occupies a large volume.

To examine the specific volume of peptides in solution, we characterized the size of IP5 via light-scattering experiments. Using static light scattering (see Figure S1 in the Supporting Information), we found that the peptide has an average molecular weight of $M \approx 16$ kg/mol, which corresponds to an IP5 oligomer with an aggregation number of 3.5. Our quasi-elastic light-scattering (QLS) experiments (Figure 2) revealed that, in solution, the peptide has a narrowly distributed apparent hydrodynamic radius (R_h). We measured R_h as a function of the peptide concentration at various temperatures (see Figure 2). The extrapolated R_h value at c = 0 (i.e., that in the indefinite dilute solution) is R_{h0} = 3.1 nm; this value is essentially independent of temperature. Assuming the specific exclusion volume of particles in question scales as $EV_s = 4\pi N_A R_{h0}^3/(3M)$, we can use this ratio to compare the critical concentrations of various proteins. (Note that, depending on the shape of the molecule, the specific exclusion volume could differ from its specific volume.) For our peptide oligomer, EV_s = 4.6 mL/g. For comparison, we determined the R_{h0} of a near-

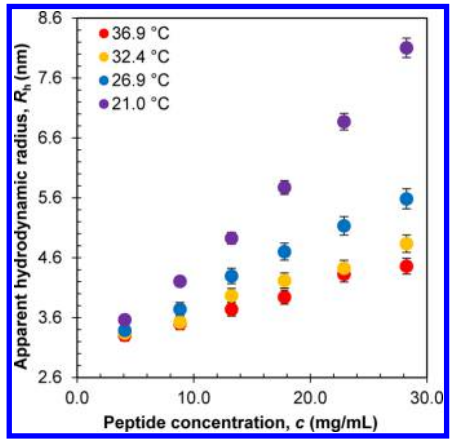

Figure 2. Apparent hydrodynamic radius (R_h) of the incretin peptide (IP5), as a function of the peptide concentration at pH 5.5 and various temperatures above the critical point.

DOI: 10.1021/acs.langmuir.7b01693
Langmuir 2017, 33, 7715−7721

spherical protein—human eye lens γD crystallin—to be given as R_{h0HgD} = 2.3 nm. The γD Crystallin has a molecular weight of M_{HgD} = 20.6 kg/mol. Our peptide oligomer has a lower molecular weight but a larger R_{h0} than the γD crystallin: $EV_{sHgD} = 4\pi N_A R_{h0HgD}^3/(3M_{HgD})$ = 1.5 mL/g. The ratio EV_s/EV_{sHgD} is ~3. Within the experimental error, this value is in good agreement with the ratio of their apparent critical volume fractions: $(\phi_c^{app})_{HgD}/\phi_c^{app}$ = 3.6.

Figure 2 also shows that the R_h of the oligomer increases as the peptide concentration increases, indicating the existence of attractive interoligomer interactions. Note that the difference in the slope (dR_h/dc) at different temperatures in Figure 2 is simply attributable to the temperature dependence of buffer viscosity. In Figure S2 in the Supporting Information, the slope dD/dc, where D is the apparent diffusion coefficient of the oligomer, is very similar at different temperatures, indicating that the strength of the interoligomer interactions is not dependent on the temperature. The results of our QLS study suggest that the peptide forms stable oligomers with sizes comparable to those of small proteins and with attractive interoligomer interactions. The molecular resemblance between the peptide oligomers and typical proteins is reflected by their similar solution behaviors.

The scaled liquid−liquid coexistence curves of the peptide oligomer and various proteins are compared in Figure 3. In this

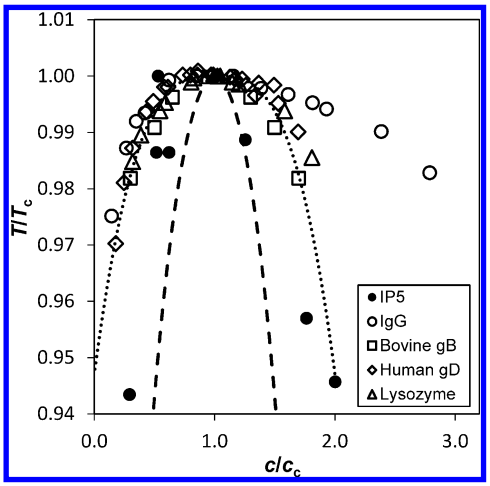

Figure 3. Scaled coexistence curves of IP5 and various proteins. The dashed curve is the theoretical curve for spherical particles with mean-field attraction calculated using the Carnahan−Starling equation of state. The dotted curve is a fit to the experimental data of bovine γB Crystallin reported in ref 29.

figure, the temperature and peptide concentration are scaled to the values at the critical point to bring the coexistence curves together and allow their shapes to be compared. The asymptotic width of the coexistence curves at the critical point (w) can be characterized using a quadratic equation:

$$w\left(\frac{T_c - T}{T}\right) = \left(\frac{c - c_c}{c_c}\right)^2$$

For spheres with mean-field interactions,[13] which are represented by the dashed curve in Figure 3, w = 6.15. For the dotted curve, which fits the data for bovine γB Crystallin,[29] w = 27. The wide coexistence curves of the near-spherical proteins are attributable to the short-range and aeolotopic (anisotropic) nature of interprotein interactions.[15] The non-spherical shape of IgG molecules is expected to result in interprotein interactions with high aeolotopicity. The experimental coexistence curves of IgGs consistently exhibit very large widths (i.e., $w \approx 120$).[8] In contrast, peptide oligomers consist of identical monomeric units; therefore, they should have more isotropic interactions. Indeed, we observed a narrow asymptotic coexistence curve for the IP5 oligomer ($w \approx 14$) in our experiments. Far from the critical point (i.e., where the concentrations exceed 100 mg/mL), the coexistence curve of the peptide in Figure 1 is flat. This feature may be attributed to the possible further growth of peptide aggregates at high concentrations. Similar coexistence curves have been observed in proteins that undergo oligomerization.[33]

LLPS in Peptide Solutions at Different pH Values. Here, we demonstrate that the LLPS of the peptide can be observed under other solution conditions, specifically, at pH >5.5. As in the case of proteins, the peptide coexistence curves should shift along the temperature axis as the interactions between oligomers change. Indeed, the coexistence curve of the peptide IP5 shifts to lower temperatures as the pH increases from 5.5 to 7.4. This peptide has an isoelectric point at pH 4.0. Therefore, as the pH increases, the net charge of the peptide increases, and the attractive interoligomer interactions decrease. At physiological pH, the phase-separation temperatures are so low that the solutions freeze before LLPS can be observed. For the same reason, LLPS is rarely observed in solutions of highly soluble proteins. Previously, we reported a method to universally observe LLPS in protein solutions by adding PEG.[8,25] The addition of PEG to protein solutions introduces extra interprotein attraction known as the depletion force.[34] The depletion force is an entropic force that increases as the protein size increases.[35] For small peptides, the depletion force is expected to be insignificant. However, peptide oligomers could be subject to PEG-induced depletion force similar to that for proteins. Indeed, the addition of PEG allows observation of LLPS in IP5 solutions at pH 7.4. We measured the phase-separation temperature of IP5 as a function of the PEG concentration (see Figure S3 in the Supporting Information) and calculated the coexistence curve at pH 7.4 (Figure 4) by extrapolating the data to a PEG concentration of zero. The

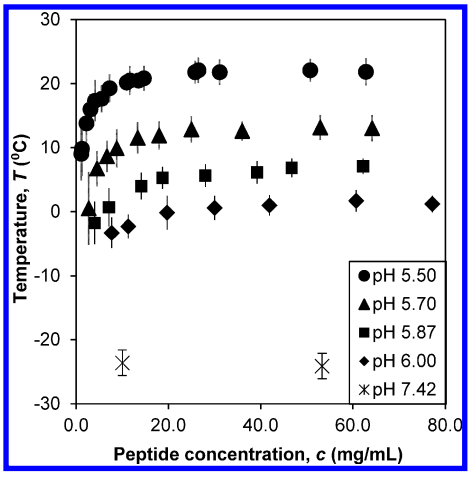

Figure 4. Coexistence curve of LLPS in solutions of IP5 at different pH values. The phase separation temperatures at pH 7.4 are below −20 °C and were indirectly determined by PEG-induced LLPS experiments.

DOI: 10.1021/acs.langmuir.7b01693
Langmuir 2017, 33, 7715−7721

linear extrapolation was experimentally validated in the PEG concentration range used in our experiments (see Figure S4 in the Supporting Information).

3. LLPS in Solutions of Different Peptides. Finally, we studied the LLPS of several peptides, including six pharmaceutical incretin peptides similar to IP5 and an anti-HIV retroviral peptide drug called enfuvirtide. IP0 is an unconjugated 40-amino acid peptide with the same sequence as the lipidated peptide IP5. IP1, IP2, IP3, IP4, and IP6 are also lipidated variants of IP0 but have different lipid conjugation sites and single-site mutations (Table S1 in the Supporting Information). Enfuvirtide is an unconjugated peptide consisting of 36 amino acids. Using PEG, we were able to observe LLPS in solutions of all these peptides at physiological pH. The propensity of each peptide to undergo phase separation depends on the energy of the effective interaction between peptide oligomers, which is evaluated as described below.

In previous studies,[25] we have shown that when phase separation occurs in dilute protein solutions, the condensed phase is essentially incompressible. Then, the protein concentration in the supernatant is, essentially, the solubility of the protein at the phase-separation temperature. In the presence of PEG, this solubility (c) is related to the osmotic pressure (Π_2) of the added PEG as follows:

$$kT \ln\left(\frac{c}{c^{\phi}}\right) = \mu_{cp} - \Pi_2 \Delta\nu$$

(see the Supporting Information for details). Here, $c^{\phi} \equiv 1$ g/L, k is the Boltzmann constant, T is the absolute temperature, and $\Delta\nu$ is a phenomenological parameter that characterizes the strength of depletion interaction. $\Delta\nu$ increases with the size of the protein. Π_2 can be calculated from the PEG concentration using a semiempirical equation (see eq S1 in the Supporting Information.[36] The parameter μ_{cp} is the protein chemical potential in the condensed phase. The energy of the effective interprotein interactions is the main contributor to μ_{cp}.

To evaluate the μ_{cp} value of different peptides, we measured the LLPS solubility of these peptides at pH 7.4 and 5 °C, as a function of the PEG3350 concentration (see Figure S5 in the Supporting Information). The logarithm of the solubility versus PEG osmotic pressure is plotted in Figure 5. This figure shows that the data of lipidated peptides are well fit by linear functions. The intercepts of the linear regression (μ_{cp}) are listed in Table 2. Generally, in the condensed phases, energetic contributions dominate entropic contributions to μ_{cp}. Here, we assume that the packing entropies of our lipidated peptides in the condensed phase are similar, because they have very similar molecular structures. Under this assumption, the μ_{cp} values determined from the plots in Figure 5 essentially reflect the energies of the interoligomer interactions of the six peptides in the condensed phase. Table 2 shows that a small change in the structure of the lipidated peptide (i.e., a single-site mutation or a change in the position of the conjugated fatty acid chain) can result in relatively large changes in the interoligomer interactions and, consequently, substantial alteration of peptide solubility. A simple explanation for this phenomenon is that changes in the peptide monomer are amplified in the oligomers by approximately the aggregation number. Therefore, we expect the phase behavior of oligomeric peptides to be more sensitive to single mutations than that of proteins. In addition, Table 2 shows the slopes of fits in Figure 5 ($N_A\Delta\nu$, where N_A is Avogadro's number). According to the depletion interaction

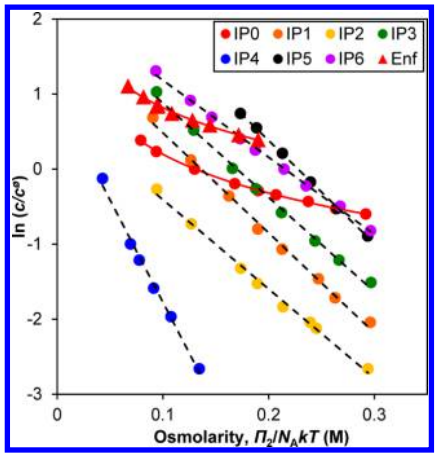

Figure 5. Logarithm of the solubility of a series of incretin peptides (IP0–IP6) and enfuvirtide (Enf) at pH 7.4 and 5 °C, as a function of the PEG3350 osmotic pressure. The dashed lines are the linear regression fits of the data. The solid red curves are visual guides for the data from unconjugated peptides (Enf and IP0).

Table 2. Chemical Potentials of the Lipidated Peptides in the Peptide-Rich Condensed Phase (μ_{cp}) and the Molar Free Volume Difference for PEG Molecules in the Two Coexisting Phases ($N_A\Delta\nu$)

	IP1	IP2	IP3	IP4	IP5	IP6
μ_{cp} (kT)	1.8	0.8	2.1	1.0	3.1	2.2
$N_A\Delta\nu$ (L/mol)	13.3	11.9	12.6	27.2	13.7	10.3

model,[34] $\Delta\nu$ characterizes the strength of the PEG-induced depletion interaction, which increases with the particle size. Thus, Table 2 indicates that oligomers of all lipidated peptides (except for IP4) have similar sizes; the larger size of the IP4 oligomer may be attributed to the electrostatic repulsion between the positive charges of the lysine residues at the N-termini of IP4 peptide chains.

The two unconjugated peptides shown in Figure 5 (IP0 and enfuvirtide) have completely unrelated amino acid sequences. However, they exhibit similar patterns of PEG-induced phase separations, which are substantially different from those of lipidated peptides. Specifically, the slopes of the unconjugated peptides in Figure 5 are relatively small and decrease as the PEG concentration increases. This behavior is consistent with the depletion interaction model. At concentrations typical for the dilute phase of our LLPS experiments (<1 mg/mL) the lipidated peptides form robust oligomers, while unconjugated peptides remain mainly monomeric. Therefore, in Figure 5, the slopes of fits for unconjugated peptides are much smaller than those for the lipidated peptides. However, as the peptide concentration increases, the unconjugated peptides begin to form labile aggregates with increased average size. Hence, the depletion force increases as peptide concentration increases. In the LLPS experiments, the peptide solubility is lower at higher PEG concentrations. Therefore, the slopes of fits for unconjugated peptides in Figure 5 decreases as PEG concentration increases.

The reversible aggregation of unconjugated peptide is also illustrated by the QLS data presented in Figure 6. Here, we observed that the lipidated peptide IP1 forms robust oligomers with R_h = 2.3 nm, which is only weakly dependent on the peptide concentration. In contrast, the R_h of the unconjugated peptide IP0 grows as its concentration increases, indicating the

DOI: 10.1021/acs.langmuir.7b01693
Langmuir 2017, 33, 7715–7721

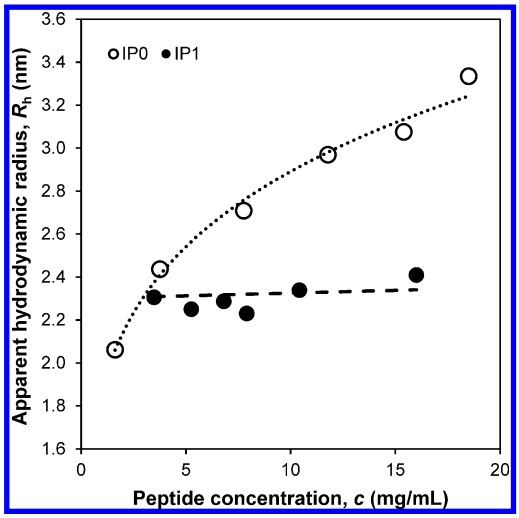

Figure 6. Apparent hydrodynamic radius (R_h) of the lipidated peptide IP1 and the unconjugated peptide IP0, as a function of the peptide concentration at pH 7.4 and 25 °C. The dashed line is a linear fit of the IP1 data. The dotted line is a quadratic fit of the IP0 data.

formation of large aggregates. Note that QLS data can only be taken at concentrations higher than that in LLPS experiments (<1 mg/mL). Figure 6 shows that, at concentration higher than ~4 mg/mL, the aggregates of IP0 grew larger than the IP1 oligomer.

CONCLUSION

In this work, we report LLPS in solutions of oligomeric peptides. The sizes of the peptide oligomers are comparable to those of globular proteins. The overall shape of the liquid–liquid coexistence curve of the peptide resembles those of globular proteins. In contrast, the apparent peptide critical volume fraction is markedly low, indicating a loose packing of the peptide in the oligomeric structures. Because the peptide oligomers contain multiple identical monomeric units, the interoligomer interactions are more isotropic than typical interprotein interactions and are sensitive to small changes in the peptide structure. We demonstrate that LLPS in oligomeric peptides is a universal phenomenon that can be revealed by adding PEG to peptide solutions and thus shifting the phase diagram into area conducive for its observation. The phase-separation temperature determined in such experiments characterizes the magnitude of the attractive interactions between peptide oligomers and ultimately their colloid stability. The study of phase transitions in protein solutions is broadly interesting to fundamental biophysics, colloidal science, and industrial applications. This work demonstrates that peptide solutions can undergo phase transitions similar to those observed in protein solutions. Future studies of peptide phase transitions will be valuable, because peptides play important physiological roles in the human body and are widely used as therapeutics.

ASSOCIATED CONTENT

Supporting Information

The Supporting Information is available free of charge on the ACS Publications website at DOI: 10.1021/acs.langmuir.7b01693.

Primary structures of the peptides studied in the work (Table S1); results of static light scattering experiment for incretin peptide IP5 (Figure S1); apparent diffusion coefficient of incretin peptide IP5, as a function of peptide concentration (Figure S2); liquid–liquid phase separation temperature of IP5 at pH 7.4, as a function of the concentration of PEG3350 (Figure S3); liquid–liquid phase-separation temperature of IP5 at a given pH (Figure S4); solubility of incretin peptides IP0–IP6 and enfuvirtide (Enf) at pH 7.4 and 5 °C (Figure S5); derivation of the equation $kT \ln(c/c^{\phi}) = \mu_{cp} - \Delta\nu\Pi_2$; and the relationship between the osmotic pressure of PEG and PEG concentration (Eq S1) (PDF)

AUTHOR INFORMATION

Corresponding Author

*Tel.: 910-962-7721. Fax: 910-962-3013. E-mail: wangyy@uncw.edu.

ORCID

Ying Wang: 0000-0001-6370-4134

Present Address

§Department of Chemistry and Biochemistry, University of North Carolina–Wilmington, 601 South College Road, Wilmington, NC 28403, USA.

Author Contributions

The manuscript was written through contributions of all authors. All authors have given approval to the final version of the manuscript.

Funding

This work is supported by the Roche Postdoctoral Fellowship (RPF) Program.

Notes

The authors declare no competing financial interest.

ACKNOWLEDGMENTS

This work is supported by the Roche Postdoctoral Fellowship (RPF) Program. We thank the Biophysical Instrumentation Facility (BIF) at MIT for the use of the Wyatt light scattering instrument. We thank Ms. Debby Pheasant at BIF for providing the technical support of the BIF instruments. We thank Dr. Arne Rufer and Mr. Eric Kusznir for the density measurements of the peptide solutions.

ABBREVIATIONS

LLPS = liquid–liquid phase separation
QLS = quasi-elastic light scattering
PEG = polyethylene glycol
EV_s = specific excluded volume

REFERENCES

(1) Gunton, J. D.; Shiryayev, A.; Pagan, D. L. *Protein Condensation: Kinetic Pathways to Crystallization and Disease*; Cambridge University Press: Cambridge and New York, 2007.

(2) Dumetz, A. C.; Chockla, A. M.; Kaler, E. W.; Lenhoff, A. M. Protein phase behavior in aqueous solutions: crystallization, liquid-liquid phase separation, gels, and aggregates. *Biophys. J.* **2008**, *94*, 570–583.

(3) Sharma, K. K.; Santhoshkumar, P. Lens aging: effects of crystallins. *Biochim. Biophys. Acta, Gen. Subj.* **2009**, *1790*, 1095–1108.

(4) Hofrichter, J.; Ross, P. D.; Eaton, W. A. Supersaturation in sickle cell hemoglobin solutions. *Proc. Natl. Acad. Sci. U. S. A.* **1976**, *73*, 3035–3039.

DOI: 10.1021/acs.langmuir.7b01693
Langmuir 2017, 33, 7715–7721

(5) Galkin, O.; Chen, K.; Nagel, R. L.; Hirsch, R. E.; Vekilov, P. G. Liquid-liquid separation in solutions of normal and sickle cell hemoglobin. *Proc. Natl. Acad. Sci. U. S. A.* **2002**, *99*, 8479−8483.
(6) Wang, Y.; Lomakin, A.; Hideshima, T.; Laubach, J. P.; Ogun, O.; Richardson, P. G.; Munshi, N. C.; Anderson, K. C.; Benedek, G. B. Pathological crystallization of human immunoglobulins. *Proc. Natl. Acad. Sci. U. S. A.* **2012**, *109*, 13359−13361.
(7) Trilisky, E.; Gillespie, R.; Osslund, T. D.; Vunnum, S. Crystallization and liquid-liquid phase separation of monoclonal antibodies and fc-fusion proteins: screening results. *Biotechnol. Progress* **2011**, *27*, 1054−1067.
(8) Wang, Y.; Lomakin, A.; Latypov, R. F.; Laubach, J. P.; Hideshima, T.; Richardson, P. G.; Munshi, N. C.; Anderson, K. C.; Benedek, G. B. Phase transitions in human IgG solutions. *J. Chem. Phys.* **2013**, *139*, 121904.
(9) McPherson, A. *Introduction to Macromolecular Crystallography*, 2nd Edition; Wiley−Blackwell: Hoboken, NJ, 2009.
(10) Ge, X.; Conley, A. J.; Brandle, J. E.; Truant, R.; Filipe, C. D. In vivo formation of protein based aqueous microcompartments. *J. Am. Chem. Soc.* **2009**, *131*, 9094−9099.
(11) Li, P.; Banjade, S.; Cheng, H. C.; Kim, S.; Chen, B.; Guo, L.; Llaguno, M.; Hollingsworth, J. V.; King, D. S.; Banani, S. F.; Russo, P. S.; Jiang, Q. X.; Nixon, B. T.; Rosen, M. K. Phase transitions in the assembly of multivalent signalling proteins. *Nature* **2012**, *483*, 336−340.
(12) Hyman, A. A.; Weber, C. A.; Julicher, F. Liquid-liquid phase separation in biology. *Annu. Rev. Cell Dev. Biol.* **2014**, *30*, 39−58.
(13) Lomakin, A.; Asherie, N.; Benedek, G. B. Monte Carlo study of phase separation in aqueous protein solutions. *J. Chem. Phys.* **1996**, *104*, 1646−1656.
(14) ten Wolde, P. R.; Frenkel, D. Enhancement of protein crystal nucleation by critical density fluctuations. *Science* **1997**, *277*, 1975−1978.
(15) Lomakin, A.; Asherie, N.; Benedek, G. B. Aeolotopic interactions of globular proteins. *Proc. Natl. Acad. Sci. U. S. A.* **1999**, *96*, 9465−9468.
(16) Anderson, V. J.; Lekkerkerker, H. N. Insights into phase transition kinetics from colloid science. *Nature* **2002**, *416*, 811−815.
(17) Kronenberg, H.; Williams, R. H. *Williams Textbook of Endocrinology*, 11th Edition; Saunders/Elsevier: Philadelphia, PA, 2008.
(18) Dutton, C. J. *Peptide Antibiotics: Discovery, Modes of Action, and Applications*; Marcel Dekker: New York, 2002.
(19) Otvos, L. *Peptide-Based Drug Design*; Humana Press: Totowa, NJ, 2008.
(20) Lewis, R. J.; Garcia, M. L. Therapeutic potential of venom peptides. *Nat. Rev. Drug Discovery* **2003**, *2*, 790−802.
(21) Kovacs, J. M.; Mant, C. T.; Hodges, R. S. Determination of intrinsic hydrophilicity/hydrophobicity of amino acid side chains in peptides in the absence of nearest-neighbor or conformational effects. *Biopolymers* **2006**, *84*, 283−297.
(22) Hartgerink, J. D.; Beniash, E.; Stupp, S. I. Peptide-amphiphile nanofibers: a versatile scaffold for the preparation of self-assembling materials. *Proc. Natl. Acad. Sci. U. S. A.* **2002**, *99*, 5133−5138.
(23) Trent, A.; Marullo, R.; Lin, B.; Black, M.; Tirrell, M. Structural properties of soluble peptide amphiphile micelles. *Soft Matter* **2011**, *7*, 9572−9582.
(24) Wang, Y.; Lomakin, A.; Kanai, S.; Alex, R.; Belli, S.; Donzelli, M.; Benedek, G. B. The molecular basis for the prolonged blood circulation of lipidated incretin peptides: peptide oligomerization or binding to serum albumin? *J. Controlled Release* **2016**, *241*, 25−33.
(25) Wang, Y.; Latypov, R. F.; Lomakin, A.; Meyer, J. A.; Kerwin, B. A.; Vunnum, S.; Benedek, G. B. Quantitative evaluation of colloidal stability of antibody solutions using PEG-induced liquid-liquid phase separation. *Mol. Pharmaceutics* **2014**, *11*, 1391−1402.
(26) Pike, E. R.; Pomeroy, W. R. M.; Vaughan, J. M. Measurement of Rayleigh ratio for several pure liquids using a laser and monitored photon counting. *J. Chem. Phys.* **1975**, *62*, 3188−3192.
(27) Fischer, H.; Polikarpov, I.; Craievich, A. F. Average protein density is a molecular-weight-dependent function. *Protein Sci.* **2004**, *13*, 2825−2828.
(28) Taratuta, V. G.; Holschbach, A.; Thurston, G. M.; Blankschtein, D.; Benedek, G. B. Liquid-liquid phase separation of aqueous lysozyme solutions: Effects of pH and salt identity. *J. Phys. Chem.* **1990**, *94*, 2140−2144.
(29) Broide, M. L.; Berland, C. R.; Pande, J.; Ogun, O. O.; Benedek, G. B. Binary-liquid phase separation of lens protein solutions. *Proc. Natl. Acad. Sci. U. S. A.* **1991**, *88*, 5660−5664.
(30) Silverton, E. W.; Navia, M. A.; Davies, D. R. Three-dimensional structure of an intact human immunoglobulin. *Proc. Natl. Acad. Sci. U. S. A.* **1977**, *74*, 5140−5144.
(31) Harris, L. J.; Larson, S. B.; Hasel, K. W.; McPherson, A. Refined structure of an intact IgG2a monoclonal antibody. *Biochemistry* **1997**, *36*, 1581−1597.
(32) Saphire, E. O.; Parren, P. W.; Pantophlet, R.; Zwick, M. B.; Morris, G. M.; Rudd, P. M.; Dwek, R. A.; Stanfield, R. L.; Burton, D. R.; Wilson, I. A. Crystal structure of a neutralizing human IGG against HIV-1: A template for vaccine design. *Science* **2001**, *293*, 1155−1159.
(33) Annunziata, O.; Pande, A.; Pande, J.; Ogun, O.; Lubsen, N. H.; Benedek, G. B. Oligomerization and phase transitions in aqueous solutions of native and truncated human beta B1-Crystallin. *Biochemistry* **2005**, *44*, 1316−1328.
(34) Asakura, S.; Oosawa, F. Interaction between particles suspended in solutions of macromolecules. *J. Polym. Sci.* **1958**, *33*, 183−192.
(35) Kulkarni, A. M.; Chatterjee, A. P.; Schweizer, K. S.; Zukoski, C. F. Effects of polyethylene glycol on protein interactions. *J. Chem. Phys.* **2000**, *113*, 9863−9873.
(36) Cohen, J. A.; Podgornik, R.; Hansen, P. L.; Parsegian, V. A. A phenomenological one-parameter equation of state for osmotic pressures of PEG and other neutral flexible polymers in good solvents. *J. Phys. Chem. B* **2009**, *113*, 3709−3714.

DOI: 10.1021/acs.langmuir.7b01693
Langmuir 2017, 33, 7715−7721